Activating transcription factor 4 modulates TGFβ-induced aggressiveness in triple negative breast cancer via SMAD2/3/4 and mTORC2 signaling

Adrián González-González[#1,2], Esperanza Muñoz-Muela[#1,2], Juan A. Marchal[3], Francisca E. Cara[1,2], Maria P. Molina[1,2], Marina Cruz-Lozano[1,2], Gema Jiménez[3], Akanksha Verma[4], Alberto Ramírez[5], Wei Qian[5], Wen Chen[5], Anthony J. Kozielski[5], Olivier Elemento[4], María D. Martín-Salvago[6], Rafael J. Luque[6], Carmen Rosa-Garrido[7], David Landeira[2,8], María Quintana-Romero[2,8], Roberto R. Rosato[5], Maria A. García[9], Cesar L. Ramirez-Tortosa[6], Hanna Kim[10], Cristian Rodriguez-Aguayo[11], Gabriel Lopez-Berestein[11], Anil K. Sood[11], Jose A. Lorente[2], Pedro Sanchez-Rovira[1,2], Jenny C. Chang[5], Sergio Granados-Principal[1,2,7].

# Contributed equally

[1]UGC Oncología Médica, Complejo Hospitalario de Jaén, Jaén, Spain.

[2]GENYO, Centre for Genomics and Oncological Research, Granada, Spain.

[3]Instituto de Biopatología y Medicina Regenerativa (IBIMER), Universidad de Granada, Granada, Spain.

[4]Institute for Computational Biomedicine, Weill Cornell Medical College, New York, NY, USA.

[5]Houston Methodist Cancer Center, Houston Methodist Hospital, Houston, TX, USA.

[6]UGC Anatomía Patológica, Complejo Hospitalario de Jaén, Jaén, Spain.

[7]FIBAO. Complejo Hospitalario de Jaén, Servicio Andaluz de Salud, Jaén, Spain.

[8]Department of Biochemistry and Molecular Biology II, Faculty of Pharmacy, University of Granada, Granada, Spain.

[9]Department of Oncology, Virgen de las Nieves University Hospital, Granada, Spain.

[10]Texas Tech University Health Sciences Center, School of Pharmacy, Amarillo, TX, USA.

[11]Center for RNA Interference and Non-Coding RNA, The University of Texas MD Anderson Cancer Center, Houston, TX, USA.

Running title: ATF4, biomarker and target in triple negative breast cancer

Keywords: ATF4, TGFβ, triple negative breast cancer, patient prognosis, personalized medicine.

Corresponding author: Sergio Granados-Principal, PhD, Complejo Hospitalario de Jaén, Avenida del Ejército Español 10, Jaén, Spain. Phone: (+34) 651 55 79 21. E-mail: sergio.granados.exts@juntadeandalucia.es

ACKNOWLEDGEMENTS

Funding was provided by Instituto de Salud Carlos III (S. Granados-Principal: CP14/00197, PI15/00336, MV16/00005; J.A. Marchal: PIE16/00045), European Regional Development Fund (S. Granados-Principal), the Chair "Doctors Galera-Requena in Cancer Stem Cell Research" (J.A. Marchal), Spanish Ministry of Economy and Competitiveness and Andalusian Regional Government (D. Landeira: RYC-2012-10019; BFU2016-75233-P; PC-0246-2017). M. Quintana-Romero is funded by the "Garantia Juvenil" program (REF-2813) (Andalusian Regional Government and University of Granada). We thank Dr. Pedro Carmona-Sánchez for the assistance on statistics of the meta-analysis and Editage (www.editage.com) for English language editing.

TRANSLATIONAL RELEVANCE

Tumor heterogeneity, metastases, and drug resistance define the aggressiveness and poor survival rates of triple-negative breast cancer (TNBC). ATF4 is overexpressed in breast cancer and TNBC, but its impact on patient survival remains unclear. We demonstrated that *ATF4* expression correlates with lower overall and relapse-free survival rates in breast cancer and TNBC patients. ATF4 has growth factor-dependent functions, which remain unclear in breast cancer. We showed *in vitro* and *in vivo* that *ATF4* depletion leads to the metastasis rate, cancer stemness, and tumor cell survival reduction through the modulation of TGFβ/SMAD and PI3K/mTOR pathways and identified a pathway-guided gene signature with prognostic potential. Differential outcomes of patients of the same cancer subtype, treated with the same therapies, demonstrate that novel biomarkers and therapeutic targets are required for the personalized treatment approach. Our findings suggest that ATF4 may serve as a prognostic biomarker and therapeutic target in TNBC patients.

ABSTRACT

Purpose. Based on the identified stress-independent cellular functions of activating transcription factor 4 (ATF4), we reported enhanced ATF4 levels in MCF10A cells treated with TGFβ1. ATF4 is overexpressed in triple negative breast cancer (TNBC) patients, but its impact on patient survival and the underlying mechanisms remain unknown. We aimed to determine *ATF4* effects on breast cancer patient survival and TNBC aggressiveness, and the relationships between TGFβ and ATF4. Defining the signaling pathways may help us identify a cell signaling-tailored gene signature.

Experimental design. Patient survival data was determined by Kaplan-Meier analysis. Relationship between TGFβ and ATF4, their effects on aggressiveness (tumor proliferation, metastasis, and stemness), and the underlying pathways were analyzed in three TNBC cell lines and *in vivo* using patient-derived xenografts (PDXs).

Results. *ATF4* overexpression correlated with TNBC patient survival decrease and a SMAD-dependent crosstalk between ATF4 and TGFβ was identified. *ATF4* expression inhibition reduced migration, invasiveness, mammosphere-forming efficiency, proliferation, epithelial-mesenchymal transition, and antiapoptotic and stemness marker levels. In PDX models, *ATF4* silencing decreased metastases, tumor growth, and relapse after chemotherapy. ATF4 was shown to be active downstream of SMAD2/3/4 and mTORC2, regulating TGFβ/SMAD and mTOR/RAC1-RHOA pathways independently of stress. We defined an eight-gene signature with prognostic potential, altered in 45% of 2509 breast cancer patients.

Conclusions. ATF4 may represent a valuable prognostic biomarker and therapeutic target in TNBC patients, and we identified a cell-signaling pathway-based gene signature that may contribute to the development of combinatorial targeted therapies for breast cancer.

INTRODUCTION

Breast cancer is the most commonly diagnosed type of cancer in women and it is associated with high incidence and death rates (1,2). Triple negative breast cancer (TNBC) is an estrogen (ER), progesterone, and HER2 receptor-negative, very aggressive form of breast cancer, with a poor survival rate. TNBC is characterized by high proliferation, heterogeneity, metastases, drug resistance, and incidence of relapse, and enriched in aggressiveness-related signaling pathways such as TGFβ or mTOR. Currently, no approved targeted therapies exist for its treatment (2,3). New or improved targeted therapies, patient stratification into responsive-to-treatment subgroups using novel prognostic biomarkers, and the identification of new therapeutic targets are required to ensure an effective personalized therapy (1).

Under stress conditions, including hypoxia, nutrient deprivation, or endoplasmic reticulum stress (ERS), the integrated stress response (ISR) is activated in cells to preserve homeostasis. The activation of the ISR leads to the global protein synthesis reduction through the eukaryotic translation initiation factor 2 alpha (eIF2α) phosphorylation, driving the translation-regulated activation of activating transcription factor 4 (ATF4) that regulates cell fate. eIF2α phosphorylation is initiated by protein kinase-like endoplasmic reticulum kinase (PERK, EIF2AK3), general control nonderepressible 2 (GCN2, EIF2AK4), protein kinase double stranded RNA-dependent (PKR, EIF2AK2), and heme-regulated inhibitor (HRI, EIF2AK1) in response to the ERS, amino acid deprivation, viral infection, and heme-deficiency, respectively (4,5).

ATF4 is a transcription factor belonging to the ATF/cyclic adenosine monophosphate response element binding protein (ATF/CREB) family, overexpressed in tumors, including breast cancer and TNBC (6–8). ATF4 regulates tumor growth, autophagy, drug resistance, and metastasis during ISR through PERK and GCN2 pathways (9–17). Independent of the cellular stress, ATF4 regulates

cell metabolism (8,18,19), osteoblast differentiation (20), drug resistance (21), invasion, and metastasis in esophageal squamous cell carcinoma (22). In the absence of stress, high ATF4 levels correlate with poorer cancer patient survival rate (22). We previously reported increased ATF4 expression in the unstressed MCF10A cells treated with TGFβ1 (23), indicating a potential TGFβ-mediated stress-independent control of ATF4 activity.

Due to these reports, we investigated whether ATF4 can regulate the TGFβ-induced aggressiveness of TNBC and affect patient survival. The identification of the relevant signaling pathway may facilitate the design of combinatorial targeted therapies and provide a gene signature that may improve personalized medicine in breast cancer.

MATERIALS AND METHODS

Supplementary Information includes Supplementary Materials and Methods, Supplementary Figure Legends and Supplementary Tables.

Bioinformatic analysis

Using the Kaplan-Meier plotter (www.kmplot.com/analysis), the effects of query genes on survival were assessed using 5143 samples from breast cancer patients. Gene expression, relapse-free (RFS) (*n*=3951) and overall survival (OS) data (*n*=1402) were obtained from Gene Expression Omnibus, European Genome-phenome Archive, and The Cancer Genome Atlas (24). Correlations, genomic and transcriptomic alterations, and their impact on patient survival were studied using OncoPrint and Kaplan-Meier analyses of 2509 breast cancer patients (25) by using cBioPortal database (26,27).

Human tissue samples

Paraffin-embedded tissue from TNBC patients (*n*=35), with pathologic information and follow-up, no previous chemo or radiotherapy, and with previous written informed consents signed by all patients, were obtained from the Jaen's node of the Biobank of the Public Health System of Andalusia (Complejo Hospitalario de Jaén, Spain). All samples and procedures were approved by the Ethical Committee for the Research of Jaén and were conducted in accordance with the Declaration of Helsinki and International Ethical Guidelines for Biomedical Research Involving Human Subjects (CIOMS).

ATF4 immunohistochemistry and scoring in TNBC patients' tumor tissue

Tumor tissue was stained for ATF4 (Abcam, ab28830) at 1:50 dilution as reported (28). ATF4 was assessed blindly by three different pathologists. Both staining intensity and extent in neoplastic cells were considered by using semiquantitative scores: A) staining intensity (granular, cytoplasmic) was graded as 0: no staining; 1+: weak, 2+: moderate, 3+: intense (Fig. 1B). B) staining extent was assigned with a value of 0-3 by the following criteria based on % of stained tumor cells: 0-25%=0; 26-50%=1; 51-75%=2; 76-100%=3. Finally, an integrated score was obtained by ponderation of the results as follows: values of staining extent were multiplied by the value of its corresponding intensity score. Therefore, score 0 was multiplied by 0, score 1+ was multiplied by 1, score 2+ was multiplied by 2, and score 3+ was multiplied by 3. The sum of these values (from 0 to 7) was the final score. Example: negative=10%, 1+=50%, 2+=30%, 3+=10% are assigned with the values 0, 1, 1, 0, respectively. ATF4 score: $(0\times0)+(1\times1)+(1\times2)+(0\times3)=3$.

Cell culture

TNBC cell lines, MDA-MB-231 and BT549, were purchased from the American Type Culture Collection, while SUM159PT cells were obtained from Asterand Bioscience. SBE (SMAD binding element) reporter-HEK293 (SBE-HEK293) cell line was purchased from BPS Bioscience.

All cells were maintained in Dulbecco's modified Eagle medium (Gibco) supplemented with 10% fetal bovine serum (Thermo Fisher Scientific) and 1% antibiotic-antimycotic (Gibco). SBE-HEK293 cells were cultured under Geneticin selection (Sigma), following the manufacturer's instructions.

Small interfering (si)RNA-mediated knockdown

The cells were transiently transfected with siRNAs targeting *ATF4* (25 nM), *SMAD2/3*, *SMAD4*, *PERK*, *PKR*, *GCN2*, *HRI*, eIF2α, *RPTOR*, *RICTOR*, *TAK1 (MAP3K7)*, and *RAS* (50 nM) using Lipofectamine RNAiMAX (Invitrogen). TGFβ1 (10 ng/mL) was added 48 h post-transfection, and the samples were incubated for 24 or 72 h, depending on the experiment.

Animal experiments

Patient-derived xenografts (PDXs)

All animal procedures were approved by the Methodist Hospital Research Institute Animal Care and Use Review Office. Experiments were conducted using two human TNBC-derived PDXs, BCM-4664 and BCM-3887 (basal intrinsic subtype) (29). PDXs were transplanted into the cleared mammary fat pad of 4-5-week-old *NOD.Cg-Prkdc*^{scid}*Il2rg*^{tm1Wjl}*/SzJ* (NSG) mice maintained in the standard conditions (28). When tumors reached 150-200 mm^3 in size, the mice were randomly assigned to four treatment groups (*n*=8/group): 1) Non-coding siRNA (SCR), 2) *ATF4*-siRNA (siRNA#2), 3) SCR plus docetaxel (Chemo+SCR, 20 mg/kg), and 4) siRNA#2 plus docetaxel (Chemo+siRNA#2, 20 mg/kg) groups. siRNAs were injected twice weekly for 6 weeks at 5 μg/mouse, and docetaxel was administered once per week on days 1, 14, and 28. Tumor volumes and body weights were recorded every 2 days. Tumors were calipered and volume was calculated as previously described (30). Mice were euthanized 24 h after the last injection and tumors were collected for further analyses. For tumor relapse, docetaxel was given at 33 mg/kg dose to BCM-

4664-bearing mice, and tumor volume was recorded until the appearance of morbidity, loss of 20% of body weight, or when tumors reached 2 cm^3 in size. The metastatic PDX model of TNBC is detailed in Supplementary Materials and Methods.

Statistical analysis

Differences between two groups were analyzed by two-tailed Student's *t*-test. Correlation between ATF4 staining and OS after diagnosis in tumor tissue of TNBC patients was analyzed by the Kaplan-Meier method and further Log-Rank test with SPSS 21.0. Patient samples were stratified by computing all ATF4 scores by a ROC curve analysis, and the best performing threshold was used as a cutoff of positive staining in the analysis. Tumor volume was assessed by two-way analysis of variance (ANOVA) and Bonferroni's post-hoc test. Median survival post-treatment in mice was analyzed using Log-Rank (Mantel-Cox) test and the hazard ratio with 95% confidence intervals were calculated. Each dead animal was assigned with a number 1, and each surviving mouse with a 0. The last day of treatment (day 42) was considered as day 0 for the survival analysis. A *P*-value <0.05 was considered significant.

RESULTS

High ATF4 expression, downstream of SMAD2/3/4, correlates with lower patient survival

High *ATF4* expression was shown to correlate with poorer OS (*n*=1402, *P*=0.0095) and RFS (*n*=3951, *P*=8.4e-6) in all breast cancer cases (All_BC), and RFS in ER^- (*n*=801, *P*=0.0058), ER^+ (*n*=2061, *P*=0.0011) and TNBC (*n*=255, *P*=0.016) patients (Fig. 1A and Suppl. Fig. 1A). We next investigated the ATF4 expression in 35 TNBC patients by IHC staining. The frequency of ATF4 positive staining was of 66% (intensity ≥1+) (Fig. 1B). Our results showed that patients with a score ≥1 (determined by ROC curve analysis and considered as positive cases for the Kaplan-

Meier analysis) (Suppl. Fig. 1B) had less OS after diagnosis (37 month) than patients with score <1 (considered as negative cases) (46 months) starting at a 24-months follow-up (Fig. 1C), however, it was not significant (P=0.125).

We previously reported increased ATF4 levels in TGFβ1-treated MCF10A cells (23). Because TNBC microenvironment is often enriched in TGFβ ligands (31), we analyzed TGFβ activation effects on ATF4 expression, and demonstrated that it increases in BT549 and SUM159PT cells treated with TGFβ1, which was abrogated by the TGFβR1 kinase inhibitor LY2157299 treatment (P<0.001. Fig. 1D), suggesting that ATF4 represents its downstream target. ATF4 expression induced by TGFβ1 and thapsigargin was similar in SUM159PT and BT549, and lower in MDA-MB-231 (Suppl. Fig. 1C). Knockdown experiments demonstrated that ATF4 is regulated by SMAD2/3/4 (Fig. 1E). To analyze whether SMAD2/3 directly regulates ATF4, we analyzed the human *ATF4* promoter region for SBEs and found the conserved CAGAC, CAGA, GTCT, GGCGC, GGCCG motifs (32) (Suppl. Fig. 1D). Careful inspection of ChIP-Seq data of SMAD2/3 in BT549 cells treated with TGFβ1 for 1.5 h (33) showed specific binding of SMAD2/3 to *SERPINE1* and *MMP2* (positive controls), *ATF4,* and the TGFβ1 responsive genes *ID1*, *JUN* and *CDKN1A* promoters, but not to *HBB* and *HPRT1* (negative controls) (Suppl. Fig. 1E). Further, we carried out ChIP-qPCR analysis in BT549 cells treated with TGFβ1 for 1.5 hours and found that SMAD2/3 bind to the *ATF4* promoter, comparable to the *SERPINE1* and *MMP2* promoters (Fig. 1F), what suggests that SMAD2/3 can bind and regulate the *ATF4* gene transcription.

To ascertain the importance of ATF4 effects on the TGFβ pathway, we inhibited *ATF4* expression and SBE activity was tested. The most effective siRNA sequence, siRNA#2 (Suppl. Fig. 2A), decreased SBE activity in HEK-293 cells (Fig. 1G), and phosphorylated (p)-SMAD2/3, SMAD2/3, and SMAD4 levels in BT549 and SUM159PT cells (Fig. 1H), indicating a positive

TGFβ feedback. In breast cancer patients, co-expression of *ATF4* and the canonical TGFβ pathway members correlated with poorer OS (P=0.0038; Fig. 1I), with a shift from positive to negative effects on survival when co-expressed with *SMAD4* or *SMAD3* in All_BC group (Fig. 1J). LOOCV results showed that *ATF4* overexpression induces a significant decrease in OS (Suppl. Table S1).

ATF4 inhibition suppresses the aggressiveness of TNBC cells

ATF4 depletion in the TNBC cells decreased their wound-healing ability independently of the treatment with TGFβ1 (Fig. 2A and Suppl. Fig. 2B). According to its capacity to silence *ATF4* (Suppl. Fig. 2A), siRNA#2 was more efficient to reduce the tumor cell migration. The migration index was reduced in BT549, SUM159PT and MDA-MB-231 cells, with TGFβ1 (41%, 50% and 45%, respectively) and without it (42%, 61% and 65%, respectively) (Fig. 2A). *ATF4* knockdown with siRNA#2 in BT549, SUM159PT and MDA-MB-231 cell lines reduced the number of invading cells with (67%, 50% and 46%, respectively) and without TGFβ1 (38%, 23% and 54%, respectively) (Fig. 2B). In absence of chemoattractant, less number of invading cells was seen upon TGFβ1 treatment in BT549 and SUM159PT cell lines (50% and 42%, respectively). Such a decrease was seen in MDA-MB-231 regardless the absence (44% decrease) or presence (55% decrease) of TGFβ1 in the medium. These changes were accompanied with the downregulation of epithelial-mesenchymal transition (EMT)-related transcription factors (ZEB1, TWIST1, SNAIL, and SLUG) in all cells after TGFβ1 treatment, and TWIST1 and SNAIL without TGFβ1. N-cadherin levels were decreased in BT549 and SUM159PT cells, but they were not detected in MDA-MB-231 cells (Fig. 2C). Cell proliferation diminished after *ATF4* knockdown (Fig. 2D), which was followed by a reduction in BCL2 and MCL1 in these cells (Fig. 2E).

Cancer stem cells (CSCs) contribute to metastasis, tumor growth, and treatment resistance. To determine whether the role of ATF4 in the TNBC aggressiveness is affected by CSC alterations,

we assessed ATF4 expression in mammospheres as a surrogate marker of CSCs *versus* the attached cells. Protein levels were shown to increase with time and mammosphere generation stage (Fig. 3A and Suppl. Fig. 2C). We investigated the effects of *ATF4* depletion on mammosphere-forming efficiency (MSFE), which was reduced after *ATF4* knockdown in all cells (Fig. 3B). Since ATF4 expression was induced by oxidative stress in suspension cultures (13), we measured the expression levels of stemness markers after *ATF4* inhibition in the attached cells, to determine whether our results were due to the modulation of stem-like properties or they represent a consequence of detachment. *NANOG*, *SOX2*, *OCT4*, and *CXCL10* levels were decreased in BT549 and SUM159PT cells (Fig. 3C). These results were confirmed at protein levels as well, except for CXCL10, which was not detected (Fig. 3D). With TGFβ1, cleaved NOTCH1, OCT4 and CD44 expression levels were consistently decreased in all cells. Without TGFβ1, NANOG, NOTCH1 and CD44 proteins were inhibited by *ATF4*-siRNA (Fig. 3D).

ATF4 inhibition reduces metastases, tumor growth, and relapse in the PDX models

We selected the BCM-3887 and BCM-4664 PDX models for our analyses, with high and medium *ATF4* expression, respectively, by RNA-Seq and IHC (Fig. 4A and B). To determine the effects of *ATF4* silencing on metastases, we used a highly metastatic PDX model (3887-LM) in mice. After the primary tumor removal, mice were treated with DOPC-conjugated *ATF4*-siRNA#2 and SCR twice weekly for 6 weeks. siRNA#2-treated animals had less metastatic nodules in liver and lungs ($P<0.05$; Fig. 4C and D). Metastatic lesions were confirmed microscopically by Ki67 staining (Fig. 4E) and they were positive for ATF4 (Fig. 4F).

We assessed tumor growth, ALDF+ subpopulation number, and recurrence following the mouse treatment with *ATF4*-siRNA and/or docetaxel. *In vivo ATF4* silencing significantly reduced the tumor growth alone ($P<0.01$) or in combination with docetaxel ($P<0.05$; Fig. 5A), while the

ALDF+ subpopulation number decreased in BCM-3887 model (Fig. 5B). In the BCM-4664 model, *ATF4* inhibition restrained the tumor growth (Fig. 5C) and the ALDF+ subpopulation number (Fig. 5D) compared with those in the controls. To investigate tumor relapse after chemotherapy, we co-administered *ATF4*-siRNA and docetaxel (33 mg/kg) twice per week for 6 weeks to mice bearing BCM-4664 tumors. Chemo+SCR tumors reached the minimum volume (124 mm^3) at day 24, while the regrowth was initiated at day 28 (128 mm^3), showing a 2.4-fold increase at day 38. In contrast, tumor volume in Chemo+siRNA#2 mice was 63 mm^3 at day 24, and they started to regrow at day 28 (78 mm^3), reaching a 1.4-fold increase at day 38. At day 56, tumor volume in Chemo+SCR was 2083 mm^3, while it was shown to reach 548 mm^3 in Chemo+siRNA#2 mice (P<0.001; Fig. 5C). Median survival post-treatment was 28 days in Chemo+siRNA#2 and 15 days in Chemo+SCR (P<0.0001; Fig. 5E). To confirm that *ATF4* targeting was successful, we determined ATF4 expression in BCM-3887 (Fig. 5F) and BCM-4664 tumors (Fig. 5G).

ATF4 is a downstream mTORC2 target and is involved in the regulation of mTOR/RAC1-RHOA in a stress-independent manner

To analyze whether TGFβ activates ISR-dependent ATF4 expression, we knocked down *PERK*, *PKR*, *GCN2*, *HRI*, and eIF2α in the presence of TGFβ1, and demonstrated that their inhibition did not downregulate ATF4 expression consistently across the cell lines (Fig. 6A). PERK, PKR and GCN2 depletion in SUM159PT cells, and GCN2 in MDA-MB-231, inhibited ATF4, indicating a cell line-dependent relevance of these pathways on ATF4 expression. Unexpectedly, ATF4 levels were increased upon eIF2α knockdown. Interestingly, after *PERK* knockdown, p-eIF2α was inhibited only in BT549 and MDA-MB-231 cells, what did not correlate with a decrease of ATF4. We inhibited the non-canonical TGFβ pathways MEK/ERK, PI3K, TAK1, and P38-MAPK (34) using the pharmacological inhibitors and TGFβ1. ATF4 expression was decreased after PI3K and

TAK1 inhibition (Suppl. Fig. 3A). PI3K, mTOR, and SGK1/2 were shown to represent the upstream ATF4 regulators, independent of AKT and PDK1 (Suppl. Fig. 3B). A second PI3K inhibitor treatment excluded possible inhibitor-dependent off-target effects on ATF4 expression (Suppl. Fig. 3C). To test whether the crosstalk between TGFβ and RAS, upstream of PI3K, represents the leading signal, we transfected BT549 and SUM159PT cells with *RAS*-siRNA, accompanied or not by the treatment with TGFβ1. *RAS* inhibition failed to decrease ATF4 levels, independent of p-AKT levels (Suppl. Fig. 3D).

Rapamycin inhibits mTORC1 and mTORC2 in a dose- and time-dependent manner, together with SGK1 expression, which is activated by mTORC2 (35). To determine whether ATF4 is a downstream target of mTORC1 and/or mTORC2 with active TGFβ, TNBC cells were transfected with *RPTOR* or *RICTOR*-siRNAs and treated with TGFβ1. We observed decreased ATF4 levels only following the *RICTOR* inhibition in all analyzed cells (Fig. 6B). Since we showed that SNAIL expression considerably decreases after *ATF4* knockdown, it was used as a surrogate for ATF4 inhibition. SNAIL levels were decreased after *RICTOR* silencing and TGFβ1 treatment in all analyzed cells (Fig. 6C).

mTOR signaling activity is modulated by several feedback loops (35), and therefore, we analyzed a potential feedback loop between ATF4 and mTORC1/2. In 2509 breast cancer patients, *ATF4* expression was shown to correlate with the expression of mTORC1 (*EIF4E*, R=0.463; *RPS6*, R=0.380) and mTORC2 targets (*NDRG1*, R=0.213; *RHOA*, R=0.320) (P<0.0001; Fig. 6D). The positive feedback between ATF4 and mTORC1 and mTORC2 activity was further confirmed by demonstrating that *ATF4*-siRNA treatment inhibited the downstream targets of mTORC2 (p-NDRG1, RHOA, RAC1) and mTORC1 pathway (p-AKT, p-P70S6K) in SUM159PT and BT549 cells (Fig. 6E). Interestingly, RHOA and RAC1 levels were consistently reduced after TGFβ1

treatment, and RAC1 expression inhibition was maintained at different time points in all cell lines (Fig. 6E and Suppl. Fig. 3E).

Collectively, our data suggest that ATF4 is involved in and regulates both the canonical, SMAD2/3/4, and non-canonical, PI3K/mTORC2/RHOA-RAC1, TGFβ signaling pathways to modulate metastasis, stemness, and tumor cell survival (Fig. 6F).

Prognostic potential of a mechanism-based gene signature in breast cancer patients

To help improve the prognosis and treatment decision-making in breast cancer patients, using Kaplan-Meier plotter database, we studied the impact of different members of the TGFβ/SMAD/ATF4 and PI3K/mTOR/ATF4 pathways on the breast cancer patient RFS (Suppl. Table S2) using multivariate analysis and LOOCV. Here, we identified an eight-gene signature, including *ATF4*, *TGFBR1*, *SMAD4*, *PIK3CA*, *RPTOR*, *EIF4EBP1*, *RICTOR*, and *NDRG1* genes, that predicts a poorer RFS in the high-expression cohort of All_BC (61-fold-change decrease; n=1764, P<0.005), ER^- (81-fold-change decrease, n=347, P<0.005) (Fig. 6G), and basal intrinsic subtype (n=618, P<0.005; Suppl. Table S3). In All_BC group, this signature predicts a 27-time poorer RFS compared with that predicted by using *ATF4* expression alone, as the single gene associated with the highest significant decrease in RFS of this group. In the ER^- group, multi-gene signature predicts a 53-time poorer RFS compared with that predicted using *NDRG1* expression alone, which was the gene associated with the highest significant decrease in the RFS of this group (P<0.005; Fig. 6G). LOOCV results demonstrated that the lower RFS in ER^+ and TNBC patients depended on the *NDRG1* expression, although its impact on RFS could not be determined in TNBC patients (P<0.008; Suppl. Table S2).

OncoPrint in 2509 breast cancer patients showed that the gene-signature expression is altered in 1138 patients (45%) (Suppl. Fig. 3F). The percentages of alterations ranged from 4%-25% for

individual genes (*ATF4*, 4%; *TGFBR1*, 4%; *SMAD4*, 7%; *PIK3CA*, 7%; *RPTOR*, 8%; *EIF4EBP1*, 16%; *RICTOR*, 6%; *NDRG1*, 25%). Kaplan-Meier analysis and LOOCV results showed that patients with the altered expressions (n=1055) of these genes have poorer survival (143 months) compared with that of the patients without alterations (n=925, 173 months, P=0.00005) (Fig. 6H).

DISCUSSION

ATF4 has been proposed as a potential contributor to the pathogenesis and development of breast cancer, however, the underlying mechanisms and the impact on patient survival remain unclear. In breast cancer patients, infiltrating carcinoma had higher p-ATF4 than normal breast tissue, what was associated with lymph node metastases (7). Recently, a gene expression analysis revealed that *ATF4* is overexpressed in TNBC patient tissues (8). Here, we investigated the potential of ATF4 as a prognostic marker and therapeutic target in breast cancer and showed that high *ATF4* RNA expression correlates with poorer survival in All_BC, ER^+, ER^-, and TNBC patients. In a cohort of 35 TNBC patients we found a trend showing that ATF4 protein expression correlates with a poorer OS. Our results demonstrate that ATF4 positiveness starts to have a negative impact on survival of TNBC patients at 24 months of follow-up. A higher follow-up period and a bigger cohort would be necessary to show statistically significant results.

During tumor invasion and metastases, active pathways like TGFβ or NOTCH induce EMT, a shift from the epithelial into mesenchymal phenotype, induced by transcription factors such as SNAIL, SLUG, TWIST1, and ZEB1 (36). TGFβ-induced EMT leads to the generation of CSCs with increased self-renewal and tumor-initiating capabilities, resistance to apoptosis and chemotherapy, decreased proliferation, and enhancing tumor recurrence (31). TNBC samples exhibit gene expression profiles observed in CSCs and during EMT, such as increased TGFβ and mTOR

expression (3), together with a more frequent expression of CSC markers, which is associated with poorer patient outcomes (37). Similar to earlier reports in osteoblasts and pancreatic adenocarcinoma cells (11,20), we reported previously enhanced ATF4 levels in MCF10A cells treated with TGFβ1 (23), which suggests that *ATF4* expression is regulated by TGFβ. This pathway is commonly upregulated and necessary in tumor progression and EMT in TNBC patients (3,31,38). Our results showed that ATF4 is expressed after TGFβ1 treatment in TNBC cells, and its expression is inhibited by the treatment with LY2157299, suggesting a direct effect of TGFβ on ATF4 expression. We showed that SMAD2/3/4 were at least partially responsible for the regulation of ATF4 expression after TGFβ1 treatment. Further analysis of previously published ChIP-Seq data (33) and subsequent ChIP-qPCR in TGFβ1-treated BT549 cells, demonstrated for the first time that SMAD2/3 bind and regulate *ATF4* transcription. Previous reports show that ATF4 was dependent of SMAD3 in mouse adipocytes (39) but independent of SMAD4 in osteoblasts (40). As previously described for ATF3 (41), *ATF4* depletion reduced TGFβ activity and SMAD2/3/4 expression, indicating the presence of a feedback loop between ATF4 and TGFβ pathway. In breast cancer patients, co-expression of *ATF4/TGFBR1*, *ATF4/SMAD2*, *ATF4/SMAD4*, and *ATF4/SMAD3* resulted in poorer OS, shown to depend on *ATF4* overexpression. Together, these results demonstrate that TGFβ/SMAD2/3/4 are upstream of ATF4, which regulate the signaling through a positive feedback with the TGFβ pathway, and it may be involved in the TGFβ-associated aggressiveness of TNBC.

Here, we report a more important role of *ATF4* in the constitutive (average of 56% decrease) than in the TGFβ1-induced tumor cell migration (average of 45% decrease). However, *ATF4* was more relevant in the TGFβ1-induced than in the basal tumor cell invasiveness (average of 54% and 38% decrease, respectively). Additionally, different EMT transcription factors and stemness markers

were inhibited by *ATF4* silencing when TGFβ1 was added or not to the medium. Our results suggest that, under non-stressing conditions, *ATF4* is involved in the aggressiveness of TNBC cells mediated not only by TGFβ, but also by other signaling pathways. In TNBC PDX mouse models, *ATF4* depletion resulted in a reduced lung and liver metastasis rate, tumor growth, ALDF+ CSC-like population numbers, delayed tumor relapse, and increased mouse survival. Accordingly, independent of the ISR-induced ATF4 expression, the effects of ATF4 on the cell functions regulated by growth-factors were shown to be important (8,18–22). Taken together, our findings indicate that ATF4 modulates the aggressiveness of TNBC through the regulation of ISR-independent key signaling pathways, suggesting a potential usefulness of this gene as a therapeutic target.

ATF4 is regulated at both transcriptional and translational levels by different signals (6). Our results show that ATF4 expression depends on the canonical SMAD-dependent TGFβ pathway, however, there are not evidences in literature showing that SMADs are responsible to modulate protein translation. Numerous stress types induce the ISR-regulated ATF4 activation mediated by p-eIF2α (4). The ISR controlled by PERK-GCN2/eIF2α/ATF4 mediates EMT and metastasis (10,11,13), tumorigenesis (9,14), and chemoresistance (16,17). In non-stressing conditions and presence of TGFβ1, we found that the ISR did not drive ATF4 expression for all the cell lines tested herein, however, it was important in SUM159PT and MDA-MB-231 cells. Contrary to previous reports (9–11,13,15,16), eIF2α depletion induced ATF4 expression and, noteworthy, when *PERK* was inhibited, reduced eIF2α phosphorylation was only observed in BT549 and MDA-MB-231, what did not reduce ATF4 levels. These results suggest that neither PERK nor eIF2α are responsible for the ATF4 translation in absence of stress and presence of TGFβ1. Therefore, we sought to investigate the eIF2α-independent regulator mechanism of ATF4

activation that could be shared by the three TNBC cell lines. TGFβ activates non-canonical pathways such as PI3K, MAPK, and TAK1 (34). Pharmacological inhibitor treatment showed that ATF4 expression in the presence of TGFβ1 is also regulated by the PI3K/mTOR pathway independent of AKT activity. In colorectal cancer, ATF4 stabilized by mutant PI3K was found downstream of PDK1/RSK2, and shown to reprogram glutamine metabolism independently of AKT (19). We showed that ATF4 expression does not depend on the presence of AKT, PDK1, RSK2, or PIK3CA mutations, as only SUM159PT cells harbored a mutation in PIK3CA (3). In contrast to previous reports (18,40), our findings revealed mTORC2 to be the leading upstream regulator of ATF4 upon TGFβ1 treatment (although mTORC1 was also important in SUM159PT and BT549 cells). mTORC2 has been reported as a necessary mediator in the TGFβ-induced EMT through AKT phosphorylation (Ser473) (42), a well-known feedback loop that activates mTORC1 (35), as well as in protein translation by direct interaction with ribosomal proteins (43). Similarly, mTORC1 modulates not only ATF4 transcription but also translation independently of eIF2α (5). Whether mTORC2 can directly regulate ATF4 translation and transcription remains elusive, but it would explain why ATF4 expression is independent of AKT, PDK1, RSK2, or PIK3CA mutations. According to previous studies (5,15), we observed that ATF4 also regulates mTOR signaling by a feedback loop on mTORC1, what may regulate cell survival and drug resistance induced by MCL1 and BCL2 (21,44), and mTORC2. We hypothesize that this dual regulation on mTOR may be attributed to the ATF4-mediated regulation of RAC1 that further affects mTORC1 and mTORC2 activity in response to growth-factor stimulation (45), which may potentiate the mTORC2/AKT feedback loop on mTORC1. Because TGFβ signaling activates both mTORC1 (46) and mTORC2 (47) in a SMAD-dependent way by inhibition of DEPTOR (47), we suggest that TGFβ could activate mTORC2 (and mTORC1 in some cell lines) through a SMAD-dependent signaling, what

would induce ATF4 expression to mediate EMT, motility, metastasis, pluripotency, and self-renewal. Active mTORC2 could also feedback on AKT to enhance mTORC1-dependent ATF4 translation and transcription. This circuit would be maintained by the feedback of ATF4 on mTOR and TGFβ signaling through the regulation of SMAD2/3/4 and mTORC1/2-RHOA-RAC1 pathways (48,49).

Identifying patterns that predict signaling pathway activation, by using gene signatures and considering the target interactions, has been demonstrated to be a viable approach to the personalized TNBC treatment (1). Since ATF4 is involved in TGFβ/SMAD and TGFβ/PI3K/mTOR pathways, we identified an eight-gene prognostic signature, including *ATF4*, *TGFBR1*, *SMAD4*, *PIK3CA*, *RPTOR*, *EIF4EBP1*, *RICTOR*, and *NDRG1* genes that can be used for the prediction of patient survival in all breast cancer, ER^-, and the basal subtype groups. The expression of these signature genes was shown to be altered in 45% of 2509 breast cancer patients, with lower survival rates observed in these patients. Breast cancer patient stratification, especially ER^- patients, according to this gene signature may provide a useful strategy for designing effective signaling pathway-guided combinatorial targeted therapies aimed at the reduction of tumor growth, metastases, and relapse risk, and may allow the identification of potentially responsive patients.

In conclusion, we demonstrate here for the first time the potential of ATF4 as a prognostic biomarker and a therapeutic target in TNBC patients. Furthermore, we showed that ATF4 is involved in the regulation of signaling pathways associated with tumor metastasis, proliferation, and drug resistance, which induce the aggressiveness of TNBC. In contrast to the previous reports, ATF4 activity was shown to be independent of the ISR, integrating and modulating TGFβ/SMAD2/3/4 and TGFβ/PI3K/mTORC1/2 pathways. We identified a signaling pathway-

guided prognostic gene signature in breast cancer patients that may help design combinatorial targeted therapies, identify potential responsive patients, and predict and overcome drug resistance. Precision medicine may benefit from our approach by improving the treatment decision-making in breast cancer patients.

REFERENCES

1. Jhan J-R, Andrechek ER. Effective personalized therapy for breast cancer based on predictions of cell signaling pathway activation from gene expression analysis. Oncogene. 2017;36:3553–61.
2. Jitariu A, Cîmpean AM, Ribatti D, Raica M. Triple negative breast cancer: the kiss of death. Oncotarget. 2017;8:46652–62.
3. Lehmann BD, Bauer JA, Chen X, Sanders ME, Chakravarthy AB, Shyr Y, et al. Identification of human triple-negative breast cancer subtypes and preclinical models for selection of targeted therapies. J Clin Invest. 2011;121:2750–67.
4. Pakos-Zebrucka K, Koryga I, Mnich K, Ljujic M, Samali A, Gorman AM. The integrated stress response. EMBO Rep. 2016;17:1374–95.
5. Park Y, Reyna-Neyra A, Philippe L, Thoreen CC. mTORC1 Balances Cellular Amino Acid Supply with Demand for Protein Synthesis through Post-transcriptional Control of ATF4. Cell Rep. 2017;19:1083–90.
6. Singleton DC, Harris AL. Targeting the ATF4 pathway in cancer therapy. Expert Opin Ther Targets. 2012;16:1189–202.
7. Fan C-F, Mao X-Y, Wang E-H. Elevated p-CREB-2 (ser 245) expression is potentially associated with carcinogenesis and development of breast carcinoma. Mol Med Rep. 2012;5:357–62.
8. van Geldermalsen M, Wang Q, Nagarajah R, Marshall AD, Thoeng A, Gao D, et al. ASCT2/SLC1A5 controls glutamine uptake and tumour growth in triple-negative basal-like breast cancer. Oncogene. 2016;35:3201–8.
9. Bobrovnikova-Marjon E, Grigoriadou C, Pytel D, Zhang F, Ye J, Koumenis C, et al. PERK

promotes cancer cell proliferation and tumor growth by limiting oxidative DNA damage. Oncogene. 2010;29:3881–95.

10. Nagelkerke A, Bussink J, Mujcic H, Wouters BG, Lehmann S, Sweep FCGJ, et al. Hypoxia stimulates migration of breast cancer cells via the PERK/ATF4/LAMP3-arm of the unfolded protein response. Breast Cancer Res. 2013;15:R2.

11. Feng Y-X, Sokol ES, Del Vecchio CA, Sanduja S, Claessen JHL, Proia TA, et al. Epithelial-to-mesenchymal transition activates PERK-eIF2α and sensitizes cells to endoplasmic reticulum stress. Cancer Discov. 2014;4:702–15.

12. Demay Y, Perochon J, Szuplewski S, Mignotte B, Gaumer S. The PERK pathway independently triggers apoptosis and a Rac1/Slpr/JNK/Dilp8 signaling favoring tissue homeostasis in a chronic ER stress Drosophila model. Cell Death Dis. 2014;5:e1452.

13. Dey S, Sayers CM, Verginadis II, Lehman SL, Cheng Y, Cerniglia GJ, et al. ATF4-dependent induction of heme oxygenase 1 prevents anoikis and promotes metastasis. J Clin Invest. 2015;125:2592–608.

14. Wu H, Wei L, Fan F, Ji S, Zhang S, Geng J, et al. Integration of Hippo signalling and the unfolded protein response to restrain liver overgrowth and tumorigenesis. Nat Commun. 2015;6:6239.

15. Liu X, Lv Z, Zou J, Liu X, Ma J, Wang J, et al. Afatinib down-regulates MCL-1 expression through the PERK-eIF2α-ATF4 axis and leads to apoptosis in head and neck squamous cell carcinoma. Am J Cancer Res. 2016;6:1708–19.

16. Dekervel J, Bulle A, Windmolders P, Lambrechts D, Van Cutsem E, Verslype C, et al. Acriflavine Inhibits Acquired Drug Resistance by Blocking the Epithelial-to-Mesenchymal Transition and the Unfolded Protein Response. Transl Oncol. 2017;10:59–69.

17. Nagasawa I, Kunimasa K, Tsukahara S, Tomida A. BRAF-mutated cells activate GCN2-mediated integrated stress response as a cytoprotective mechanism in response to vemurafenib. Biochem Biophys Res Commun. 2017;482:1491–7.

18. Ben-Sahra I, Hoxhaj G, Ricoult SJH, Asara JM, Manning BD. mTORC1 induces purine synthesis through control of the mitochondrial tetrahydrofolate cycle. Science. 2016;351:728–33.

19. Hao Y, Samuels Y, Li Q, Krokowski D, Guan B-J, Wang C, et al. Oncogenic PIK3CA mutations reprogram glutamine metabolism in colorectal cancer. Nat Commun. 2016;7:11971.

20. Lian N, Lin T, Liu W, Wang W, Li L, Sun S, et al. Transforming growth factor β suppresses osteoblast differentiation via the vimentin activating transcription factor 4 (ATF4) axis. J Biol Chem. 2012;287:35975–84.

21. Zhu H, Xia L, Zhang Y, Wang H, Xu W, Hu H, et al. Activating transcription factor 4 confers a multidrug resistance phenotype to gastric cancer cells through transactivation of SIRT1 expression. PLoS One. 2012;7:e31431.

22. Zhu H, Chen X, Chen B, Chen B, Song W, Sun D, et al. Activating transcription factor 4 promotes esophageal squamous cell carcinoma invasion and metastasis in mice and is associated with poor prognosis in human patients. PLoS One. 2014;9:e103882.

23. Granados-Principal S, Liu Y, Guevara ML, Blanco E, Choi DS, Qian W, et al. Inhibition of iNOS as a novel effective targeted therapy against triple-negative breast cancer. Breast Cancer Res. 2015;17:25.

24. Győrffy B, Lanczky A, Eklund AC, Denkert C, Budczies J, Li Q, et al. An online survival analysis tool to rapidly assess the effect of 22,277 genes on breast cancer prognosis using

551 microarray data of 1,809 patients. Breast Cancer Res Treat. 2010;123:725–31.
552 25. Pereira B, Chin S-F, Rueda OM, Vollan H-KM, Provenzano E, Bardwell HA, et al. The
553 somatic mutation profiles of 2,433 breast cancers refines their genomic and transcriptomic
554 landscapes. Nat Commun. 2016;7:11479.
555 26. Cerami E, Gao J, Dogrusoz U, Gross BE, Sumer SO, Aksoy BA, et al. The cBio cancer
556 genomics portal: an open platform for exploring multidimensional cancer genomics data.
557 Cancer Discov. 2012;2:401–4.
558 27. Gao J, Aksoy BA, Dogrusoz U, Dresdner G, Gross B, Sumer SO, et al. Integrative analysis
559 of complex cancer genomics and clinical profiles using the cBioPortal. Sci Signal.
560 2013;6:pl1.
561 28. Dave B, Granados-Principal S, Zhu R, Benz S, Rabizadeh S, Soon-Shiong P, et al. Targeting
562 RPL39 and MLF2 reduces tumor initiation and metastasis in breast cancer by inhibiting
563 nitric oxide synthase signaling. Proc Natl Acad Sci U S A. 2014;111:8838–43.
564 29. Zhang X, Claerhout S, Prat A, Dobrolecki LE, Petrovic I, Lai Q, et al. A renewable tissue
565 resource of phenotypically stable, biologically and ethnically diverse, patient-derived
566 human breast cancer xenograft models. Cancer Res. 2013;73:4885–97.
567 30. Choi DS, Blanco E, Kim Y-S, Rodriguez AA, Zhao H, Huang TH-M, et al. Chloroquine
568 eliminates cancer stem cells through deregulation of Jak2 and DNMT1. Stem Cells.
569 2014;32:2309–23.
570 31. Bhola NE, Balko JM, Dugger TC, Kuba MG, Sánchez V, Sanders M, et al. TGF-β inhibition
571 enhances chemotherapy action against triple-negative breast cancer. J Clin Invest.
572 2013;123:1348–58.
573 32. Martin-Malpartida P, Batet M, Kaczmarska Z, Freier R, Gomes T, Aragón E, et al.

574 Structural basis for genome wide recognition of 5-bp GC motifs by SMAD transcription
575 factors. Nat Commun. 2017;8:2070.
576 33. Sundqvist A, Morikawa M, Ren J, Vasilaki E, Kawasaki N, Kobayashi M, et al. JUNB
577 governs a feed-forward network of TGFβ signaling that aggravates breast cancer invasion.
578 Nucleic Acids Res. 2018;46:1180–95.
579 34. Bierie B, Moses HL. Tumour microenvironment: TGFbeta: the molecular Jekyll and Hyde
580 of cancer. Nat Rev Cancer. 2006;6:506–20.
581 35. Efeyan A, Sabatini DM. mTOR and cancer: many loops in one pathway. Curr Opin Cell
582 Biol. 2010;22:169–76.
583 36. Kalluri R, Weinberg RA. The basics of epithelial-mesenchymal transition. J Clin Invest.
584 2009;119:1420–8.
585 37. Idowu MO, Kmieciak M, Dumur C, Burton RS, Grimes MM, Powers CN, et al.
586 CD44(+)/CD24(-/low) cancer stem/progenitor cells are more abundant in triple-negative
587 invasive breast carcinoma phenotype and are associated with poor outcome. Hum Pathol.
588 2012;43:364–73.
589 38. Jovanović B, Beeler JS, Pickup MW, Chytil A, Gorska AE, Ashby WJ, et al. Transforming
590 growth factor beta receptor type III is a tumor promoter in mesenchymal-stem like triple
591 negative breast cancer. Breast Cancer Res. 2014;16:R69.
592 39. Liu Z, Gu H, Gan L, Xu Y, Feng F, Saeed M, et al. Reducing Smad3/ATF4 was essential
593 for Sirt1 inhibiting ER stress-induced apoptosis in mice brown adipose tissue. Oncotarget.
594 2017;8:9267–79.
595 40. Karner CM, Lee S-Y, Long F. Bmp Induces Osteoblast Differentiation through both Smad4
596 and mTORC1 Signaling. Mol Cell Biol. 2017;37:1–12.

41. Yin X, Wolford CC, Chang Y-S, McConoughey SJ, Ramsey S a, Aderem A, et al. ATF3, an adaptive-response gene, enhances TGF{beta} signaling and cancer-initiating cell features in breast cancer cells. J Cell Sci. 2010;123:3558–65.

42. Lamouille S, Connolly E, Smyth JW, Akhurst RJ, Derynck R. TGF-β-induced activation of mTOR complex 2 drives epithelial-mesenchymal transition and cell invasion. J Cell Sci. 2012;125:1259–73.

43. Oh WJ, Wu C, Kim SJ, Facchinetti V, Julien L-A, Finlan M, et al. mTORC2 can associate with ribosomes to promote cotranslational phosphorylation and stability of nascent Akt polypeptide. EMBO J. 2010;29:3939–51.

44. Pugazhenthi S, Nesterova A, Sable C, Heidenreich KA, Boxer LM, Heasley LE, et al. Akt/protein kinase B up-regulates Bcl-2 expression through cAMP-response element-binding protein. J Biol Chem. 2000;275:10761–6.

45. Saci A, Cantley LC, Carpenter CL. Rac1 regulates the activity of mTORC1 and mTORC2 and controls cellular size. Mol Cell. 2011;42:50–61.

46. Das R, Xu S, Nguyen TT, Quan X, Choi S-K, Kim S-J, et al. Transforming Growth Factor β1-induced Apoptosis in Podocytes via the Extracellular Signal-regulated Kinase-Mammalian Target of Rapamycin Complex 1-NADPH Oxidase 4 Axis. J Biol Chem. 2015;290:30830–42.

47. Das F, Ghosh-Choudhury N, Bera A, Dey N, Abboud HE, Kasinath BS, et al. Transforming growth factor β integrates Smad 3 to mechanistic target of rapamycin complexes to arrest deptor abundance for glomerular mesangial cell hypertrophy. J Biol Chem. 2013;288:7756–68.

48. Gulhati P, Bowen KA, Liu J, Stevens PD, Rychahou PG, Chen M, et al. mTORC1 and

mTORC2 regulate EMT, motility, and metastasis of colorectal cancer via RhoA and Rac1 signaling pathways. Cancer Res. 2011;71:3246–56.

49. Yu JSL, Cui W. Proliferation, survival and metabolism: the role of PI3K/AKT/mTOR signalling in pluripotency and cell fate determination. Development. 2016;143:3050–60.

Figure Legends

Figure 1. *ATF4* expression correlates with poor patient survival and SMAD-dependent TGFβ signaling. A) Kaplan-Meier showing that high *ATF4* expression correlates with poorer overall (OS) (*n*=1402) and relapse-free survival (RFS) in all breast cancer (All_BC, *n*=3951), estrogen receptor negative (ER^-, *n*=801) and triple negative breast cancer patients (TNBC, *n*=255). Follow-up threshold was set at 10 years. **B)** Representative images of negative, 1+, 2+, and 3+ ATF4 staining intensity in TNBC patients' tumor tissue (original optical objective: 20X). **C)** Kaplan-Meier analysis showing the impact of ATF4 staining on the OS after diagnosis of TNBC patients' tumor tissue (*n*=35). **D)** RT-PCR and western blot of ATF4 in BT549 and SUM159PT cells treated with TGFβ1 (10 ng/mL), LY2157299 (5 µM) and combination for 72 h. Inhibitor was added 1 h before TGFβ1. **E)** Western blot of ATF4 in BT549 and SUM159PT cells transfected with *SMAD2/3* and *SMAD4*-siRNAs. TGFβ1 was added 48 h after transfection for 24 h. **F)** Binding of SMAD2/3 to the *ATF4* promoter region in BT549 cells upon TGFβ1 treatment for 1.5 h was assayed by ChIP-qPCR. Values are expressed relative to input for the promoter regions of SMAD2/3 bound-genes (*SERPINE1*, *MMP2*), negative controls (*LAMB3*, *HPRT*) and *ATF4*. IgG was used as a non-specific binding control. **G)** SBE reporter assay in SBE-HEK293 cells after *ATF4* knockdown with/without TGFβ1 for 24 h. RLU: Relative Light Units. **H)** Effect of ATF4 knockdown following treatment with TGFβ1 for 24 h and 72 h on SMAD2/3 and SMAD4, respectively. Two targeted *ATF4*-siRNAs (siRNA#1 and siRNA#2) were used in BT549. siRNA#2 was the most efficient and further used in SUM159PT cells. **I)** Changes in OS of breast cancer patients when *ATF4* (*n*=1402), *SMAD2* (*n*=626), *SMAD3* (*n*=1402), *SMAD4* (*n*=626) and *TGFBR1* (*n*=626) are expressed alone or co-expressed. Survival fold change was tested by multiple

testing correction (* P<0.0038). **J)** Kaplan-Meier showing breast cancer patient OS when *ATF4* is co-expressed with *SMAD2*, *SMAD3* or *SMAD4*. HR: Hazard Ratio. *** P<0.001.

Figure 2. *ATF4* silencing inhibits the metastatic and proliferative properties of tumor cells and correlates with less expression of EMT and pro-survival markers. A) Migration and **B)** invasion of BT549, SUM159PT and MDA-MB-231 cells after *ATF4* knockdown treated with/without TGFβ1 for 24 h (MDA-MB-231 for 72 h). **C)** Changes in protein expression of EMT markers (N-cadherin, ZEB1, SNAIL, SLUG, TWIST1) after *ATF4* silencing in BT549, SUM159PT and MDA-MB-231 cells with and without TGFβ1 for 24 h. **D)** Proliferation after *ATF4* knockdown with/without TGFβ1 for 24 h (MDA-MB-231 for 72 h). **E)** Western blot analysis of pro-survival proteins (BCL2 and MCL1) after transfection with *ATF4*-siRNA#2 and treatment with TGFβ1 for 72 h. * P<0.05, ** P<0.01, ***P<0.001.

Figure 3. Mammosphere formation is decreased after *ATF4* knockdown and correlates with lower stemness markers expression. A) Increased ATF4 protein expression in primary and secondary mammosphere generations (1MS and 2MS, respectively) compared with attached (Att.) cells. **B)** Mammosphere-forming efficiency (MSFE) in three TNBC cell lines after *ATF4* inhibition and treatment with TGFβ1 for 24 h. **C)** mRNA expression of *NANOG*, *SOX2*, *OCT4*, *NOTCH1* and *CXCL10* after *ATF4* knockdown and treatment with TGFβ1 for 72 h in BT549 and SUM159PT cells in adherent conditions. **D)** Western blot of stemness markers after *ATF4* silencing and treatment with TGFβ1 for 24 h (BT549, MDA-MB-231) and 72 h (SUM159PT). * P<0.05, ** P<0.01, ***P<0.001.

Figure 4. *ATF4* targeting reduces liver and lung metastases in the PDX model 3887-LM. A) *ATF4* mRNA levels in 20 different TNBC PDX models by RNA-sequencing. **B)** Representative images of ATF4 IHC staining of BCM-3887 and BCM-4664 PDX tumor tissues (original optical

objective: 20X). **C)** Representative images and percentage of mice (*n*=5/group) with liver and **D)** lung metastases, after treatment with *ATF4*-siRNA#2 and SCR (control) for 6 weeks. **E)** Immunohistochemical assessment of liver and lung metastases by Ki67 staining (original optical objectives: 4X and 20X). **F)** Representative images of ATF4 IHC staining of liver and lung metastases (original optical objectives: 4X and 20X).

Figure 5. *ATF4* inhibition delays PDX tumor growth, cancer stem cell population number, tumor relapse and widens post-treatment survival. A) Volume of BCM-3887 tumors (*n*=8/group) treated with siRNA#2 and SCR with and without docetaxel (20 mg/kg). **B)** Flow cytometric analysis of Aldefluor-positive (ALDF+) subpopulation after *ATF4* knockdown and treatment with/without docetaxel in BCM-3387 tumor tissue. **C)** Volume of BCM-4664 tumors (*n*=8/group) treated with siRNA#2 and SCR. Co-treatment of siRNAs with docetaxel (33 mg /kg) for 6 weeks was used to study tumor relapse after treatment. The arrow indicates the end of treatment. **D)** ALDF+ subpopulation after *ATF4* knockdown in BCM-4664 tumors. **E)** Kaplan-Meier curve of median survival post-treatment in BCM-4664-bearing mice after *ATF4* knockdown in combination with docetaxel (33 mg/kg), P=0.0001. **F)** Western blot and densitometric analysis showing *ATF4* knockdown efficiency in BCM-3387 and **G)** BCM-4664 tumor tissues (*n*=5/PDX). * P<0.05, ** P<0.01, ***P<0.001.

Figure 6. The TGFβ-induced mTORC2 is the upstream regulator of ATF4 complementary to TGFβ/SMAD signaling. Prognostic potential of a mechanism-based gene signature in breast cancer patients. A) Western blot of ATF4 in cells transfected with siRNA for typical integrated-stress-response (ISR) mediators and treated with TGFβ1 for 72 h. **B)** ATF4 protein levels after knockdown of *RPTOR* and *RICTOR* treated with TGFβ1 for 72 h (SUM159PT, BT549) or 24 h (MDA-MB-231). *TAK1*-siRNA was also tested in SUM159PT. **C)** Change in SNAIL

711 expression by *RPTOR* and *RICTOR*-siRNAs in three cell lines treated with TGFβ1 for 24 h. **D)**
712 Pearson's correlation of *ATF4* mRNA expression with components of mTORC2 (*NDRG1, RHOA*)
713 and mTORC1 (*RPS6, EIF4E*) signaling in a cohort of 2509 breast cancer patients. **E)** Western blot
714 of mTORC2 and mTORC1 components in cells transfected with *ATF4*-siRNA and treated with
715 TGFβ1 for 72 h (SUM159PT cells were treated for 24 h to test for mTORC1 signaling). **F)**
716 Schematic showing the upstream regulators, the positive feedbacks detected, the downstream
717 targets of ATF4, and its corresponding biological effects that modulate TNBC aggressiveness upon
718 activation of TGFβ which are conserved in the three TNBC cell lines tested. **G)** Prognostic value
719 (RFS fold change) of the eight-gene signature *versus* each-single-gene in all (All_BC) and ER^-
720 breast cancer patients. Survival fold change was tested by multiple testing correction (* $P<0.005$)
721 and leave-one-out cross-validation. **H)** Impact of the eight-gene signature on the survival of breast
722 cancer patients with alterations in DNA (amplification, deletion) and RNA expression (up- and
723 downregulation) of each gene. Every gene was tested by leave-one-out cross-validation.

FIGURE 1

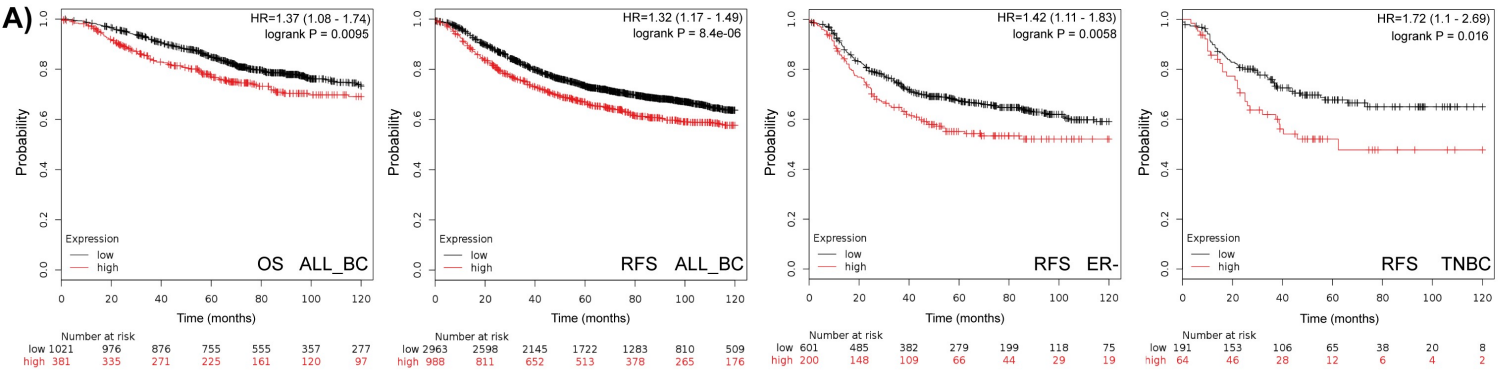
A)
HR=1.37 (1.08 - 1.74)
logrank P = 0.0095
OS ALL_BC
HR=1.32 (1.17 - 1.49)
logrank P = 8.4e-06
RFS ALL_BC
HR=1.42 (1.11 - 1.83)
logrank P = 0.0058
RFS ER-
HR=1.72 (1.1 - 2.69)
logrank P = 0.016
RFS TNBC
Probability
Time (months)
Expression
low
high
Number at risk

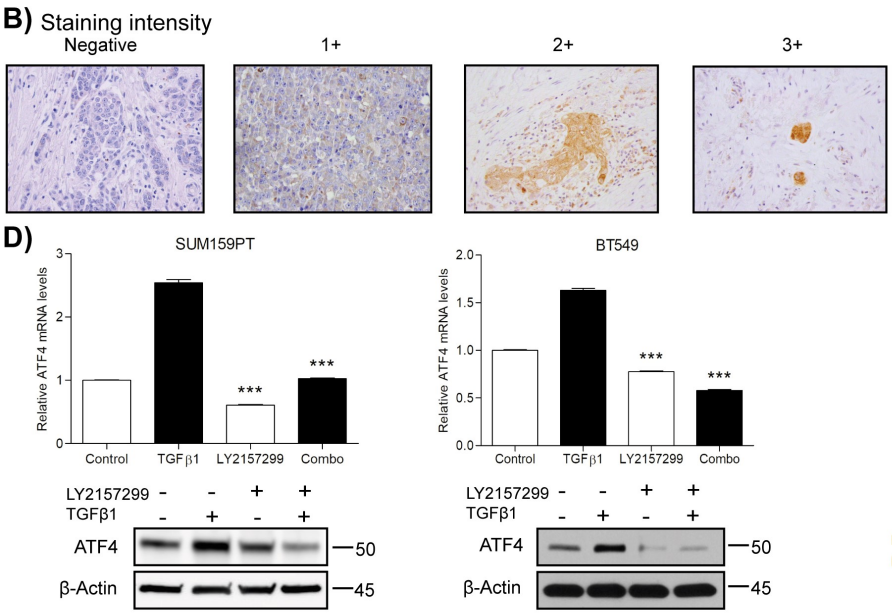
B) Staining intensity
Negative
1+
2+
3+
D)
SUM159PT
BT549
Relative ATF4 mRNA levels
Control
TGFβ1
LY2157299
Combo
LY2157299
TGFβ1
ATF4
β-Actin
50
45

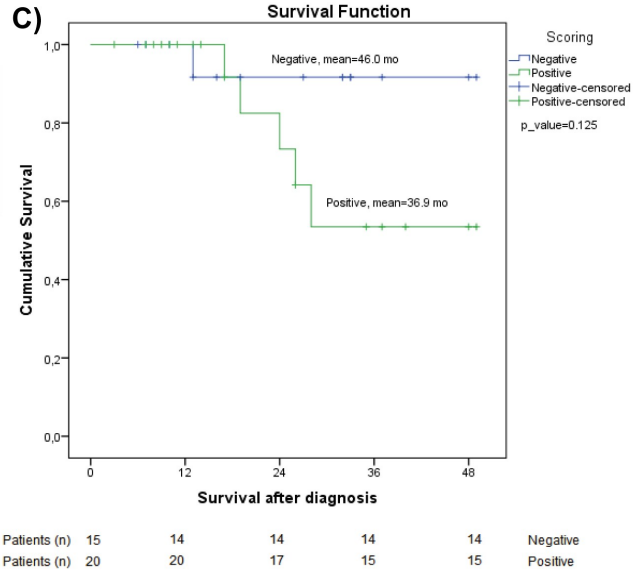
C)
Survival Function
Scoring
Negative
Positive
Negative-censored
Positive-censored
p_value=0.125
Negative, mean=46.0 mo
Positive, mean=36.9 mo
Cumulative Survival
Survival after diagnosis
Patients (n) 15 14 14 14 14 Negative
Patients (n) 20 20 17 15 15 Positive

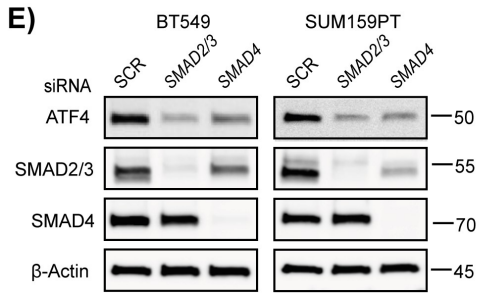
E)
BT549
SUM159PT
siRNA
SCR
SMAD2/3
SMAD4
ATF4
SMAD2/3
SMAD4
β-Actin
50
55
70
45

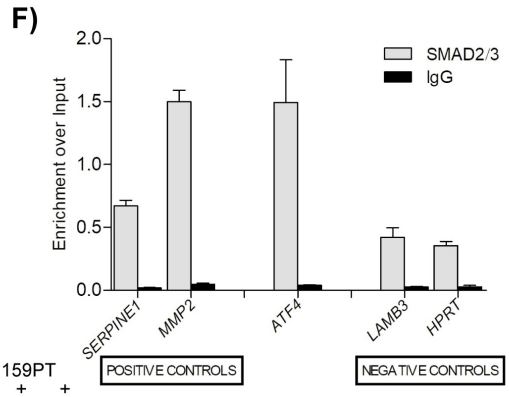
F)
SMAD2/3
IgG
Enrichment over Input
SERPINE1
MMP2
ATF4
LAMB3
HPRT
POSITIVE CONTROLS
NEGATIVE CONTROLS

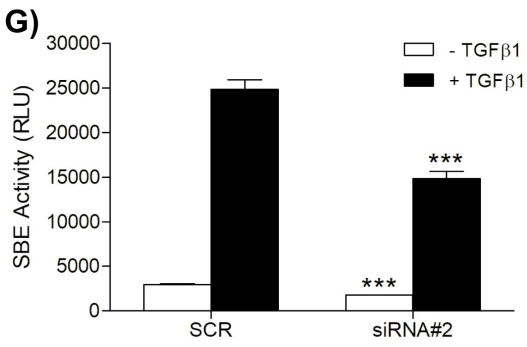
G)
- TGFβ1
+ TGFβ1
SBE Activity (RLU)
SCR
siRNA#2

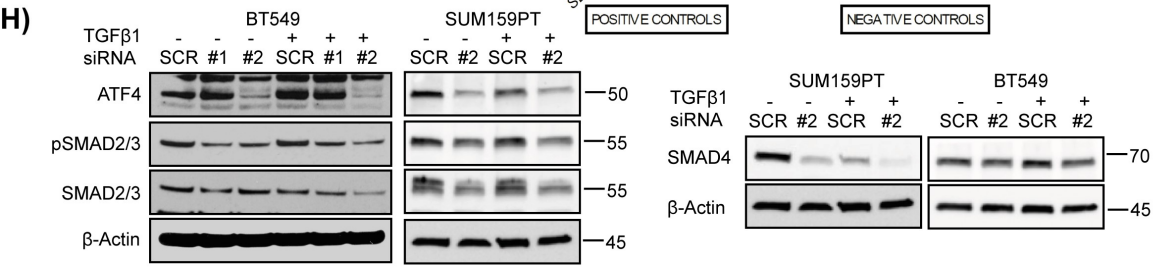
H)
BT549
SUM159PT
TGFβ1
siRNA
SCR #1 #2 SCR #1 #2
SCR #2 SCR #2
ATF4
pSMAD2/3
SMAD2/3
β-Actin
50
55
55
45
SUM159PT
BT549
TGFβ1
siRNA
SCR #2 SCR #2
SCR #2 SCR #2
SMAD4
β-Actin
70
45

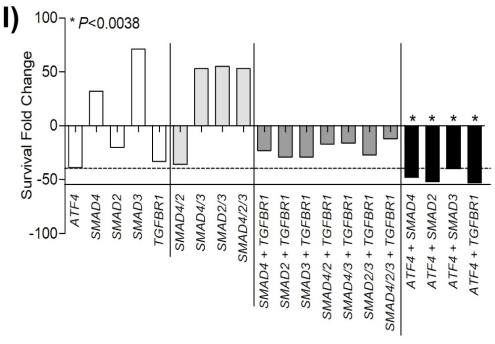
I)
* P<0.0038
Survival Fold Change
ATF4
SMAD4
SMAD2
SMAD3
TGFBR1
SMAD4/2
SMAD4/3
SMAD2/3
SMAD4/2/3
SMAD4 + TGFBR1
SMAD2 + TGFBR1
SMAD3 + TGFBR1
SMAD4/2 + TGFBR1
SMAD4/3 + TGFBR1
SMAD2/3 + TGFBR1
SMAD4/2/3 + TGFBR1
ATF4 + SMAD4
ATF4 + SMAD2
ATF4 + SMAD3
ATF4 + TGFBR1

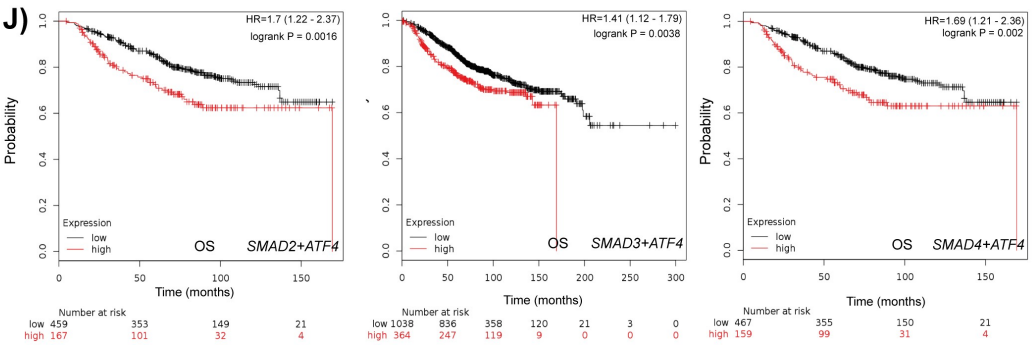
J)
HR=1.7 (1.22 - 2.37)
logrank P = 0.0016
OS SMAD2+ATF4
HR=1.41 (1.12 - 1.79)
logrank P = 0.0038
OS SMAD3+ATF4
HR=1.69 (1.21 - 2.36)
logrank P = 0.002
OS SMAD4+ATF4
Probability
Time (months)
Expression
low
high
Number at risk

FIGURE 2

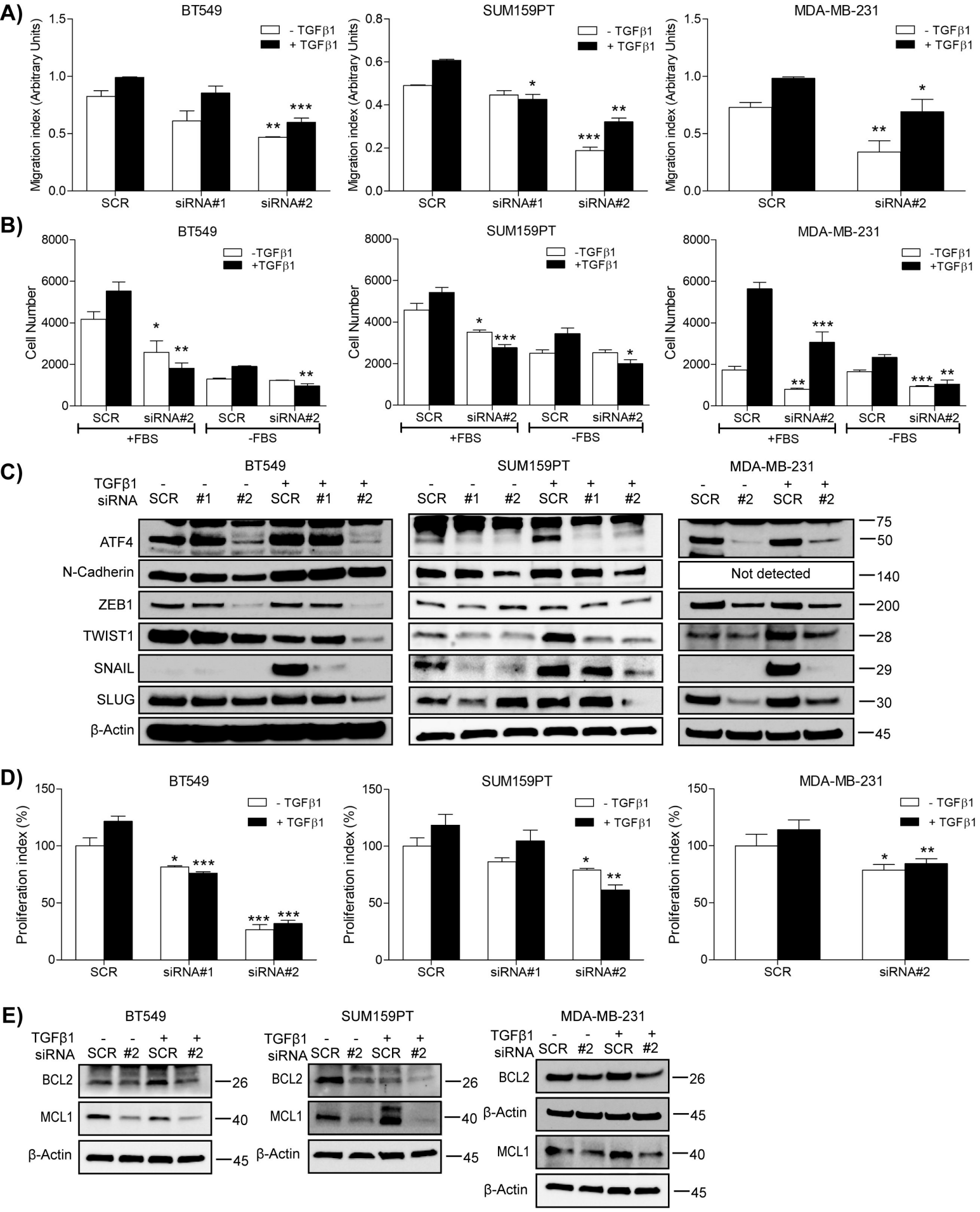
A)
BT549
SUM159PT
MDA-MB-231
- TGFβ1
+ TGFβ1
Migration index (Arbitrary Units)
SCR
siRNA#1
siRNA#2
B)
-TGFβ1
+TGFβ1
Cell Number
+FBS
-FBS
C)
TGFβ1
siRNA
SCR
#1
#2
ATF4
N-Cadherin
ZEB1
TWIST1
SNAIL
SLUG
β-Actin
Not detected
75
50
140
200
28
29
30
45
D)
Proliferation index (%)
E)
BCL2
MCL1
β-Actin
26
40
45

FIGURE 3

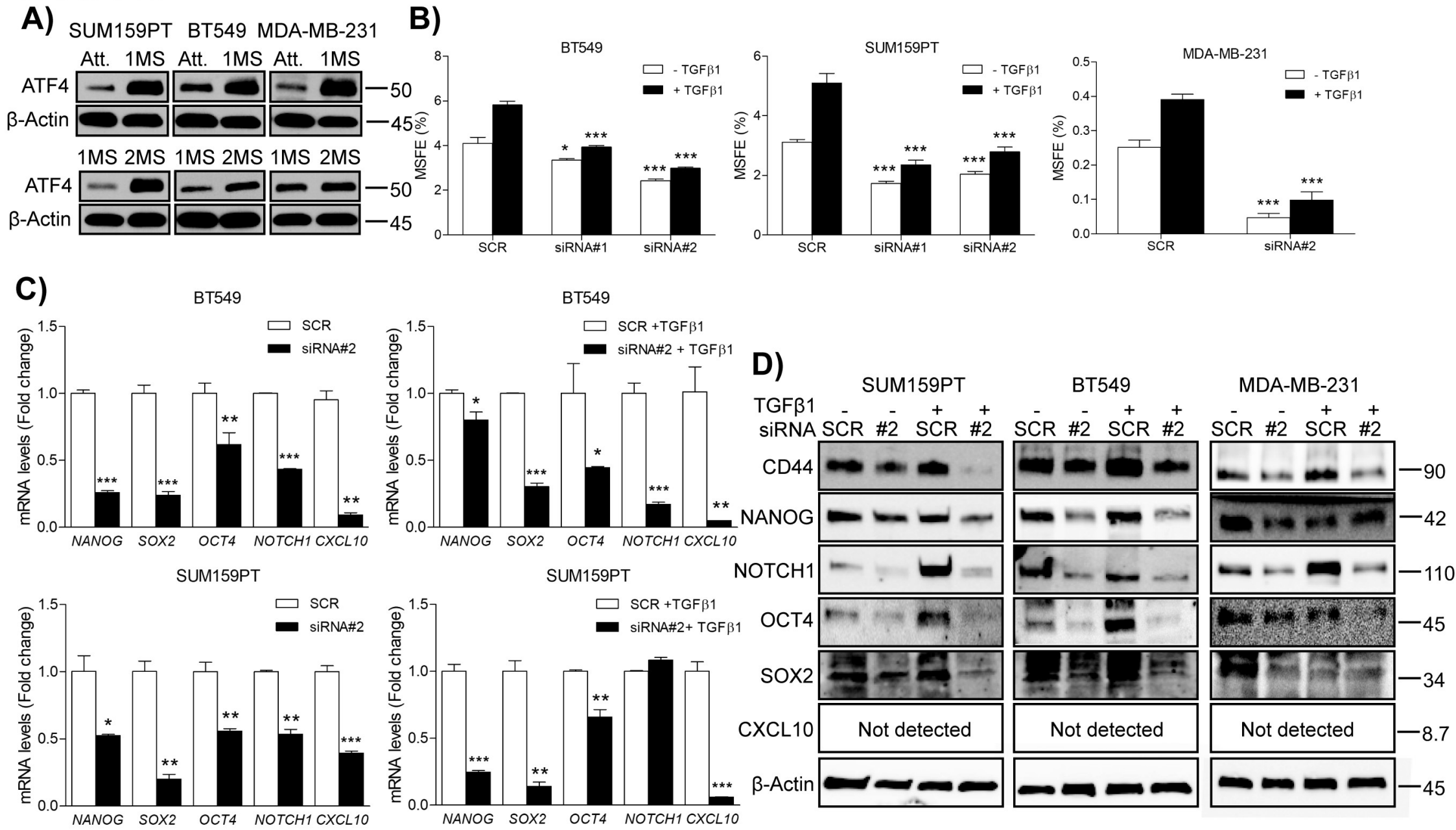
A)
SUM159PT
BT549
MDA-MB-231
Att.
1MS
ATF4
β-Actin
50
45
1MS
2MS
B)
BT549
SUM159PT
MDA-MB-231
- TGFβ1
+ TGFβ1
MSFE (%)
SCR
siRNA#1
siRNA#2
C)
BT549
SUM159PT
SCR
siRNA#2
SCR +TGFβ1
siRNA#2 + TGFβ1
siRNA#2+ TGFβ1
mRNA levels (Fold change)
NANOG
SOX2
OCT4
NOTCH1
CXCL10
D)
TGFβ1
siRNA
SCR
#2
CD44
NANOG
NOTCH1
OCT4
SOX2
CXCL10
Not detected
β-Actin
90
42
110
45
34
8.7
45

FIGURE 4

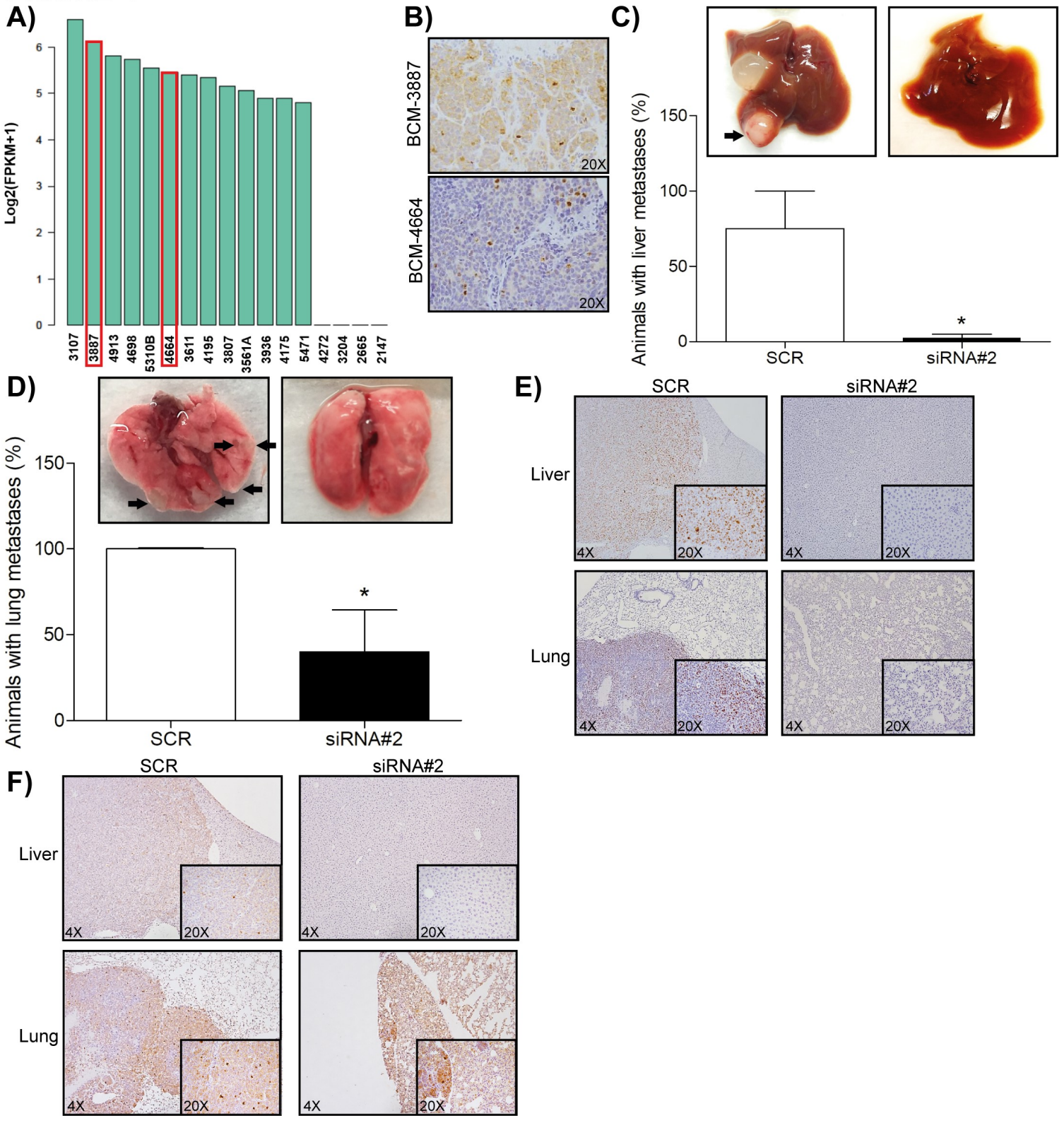
A)
Log2(FPKM+1)
0
1
2
3
4
5
6
3107
3887
4913
4698
5310B
4664
3611
4195
3807
3561A
3936
4175
5471
4272
3204
2665
2147
B)
BCM-3887
20X
BCM-4664
20X
C)
Animals with liver metastases (%)
0
50
100
150
*
SCR
siRNA#2
D)
Animals with lung metastases (%)
0
50
100
150
*
SCR
siRNA#2
E)
SCR
siRNA#2
Liver
Lung
4X
20X
F)
SCR
siRNA#2
Liver
Lung
4X
20X

FIGURE 5

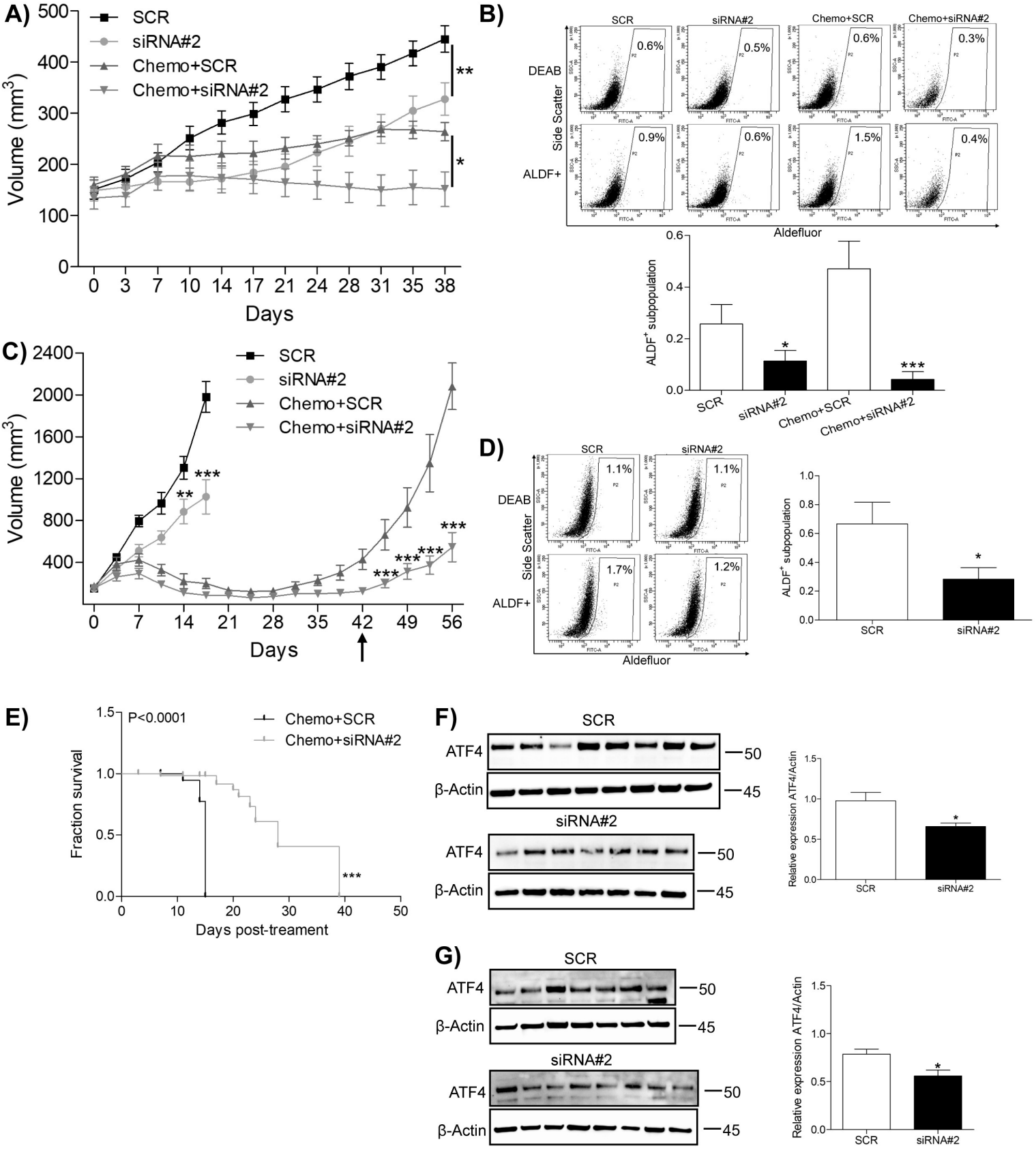
A)
SCR
siRNA#2
Chemo+SCR
Chemo+siRNA#2
Volume (mm3)
Days
B)
SCR
siRNA#2
Chemo+SCR
Chemo+siRNA#2
DEAB
ALDF+
Side Scatter
Aldefluor
0.6%
0.5%
0.6%
0.3%
0.9%
0.6%
1.5%
0.4%
ALDF+ subpopulation
C)
Volume (mm3)
Days
D)
1.1%
1.1%
1.7%
1.2%
ALDF+ subpopulation
E)
P<0.0001
Chemo+SCR
Chemo+siRNA#2
Fraction survival
Days post-treament
F)
SCR
siRNA#2
ATF4
β-Actin
Relative expression ATF4/Actin
G)
SCR
siRNA#2
ATF4
β-Actin
Relative expression ATF4/Actin

FIGURE 6

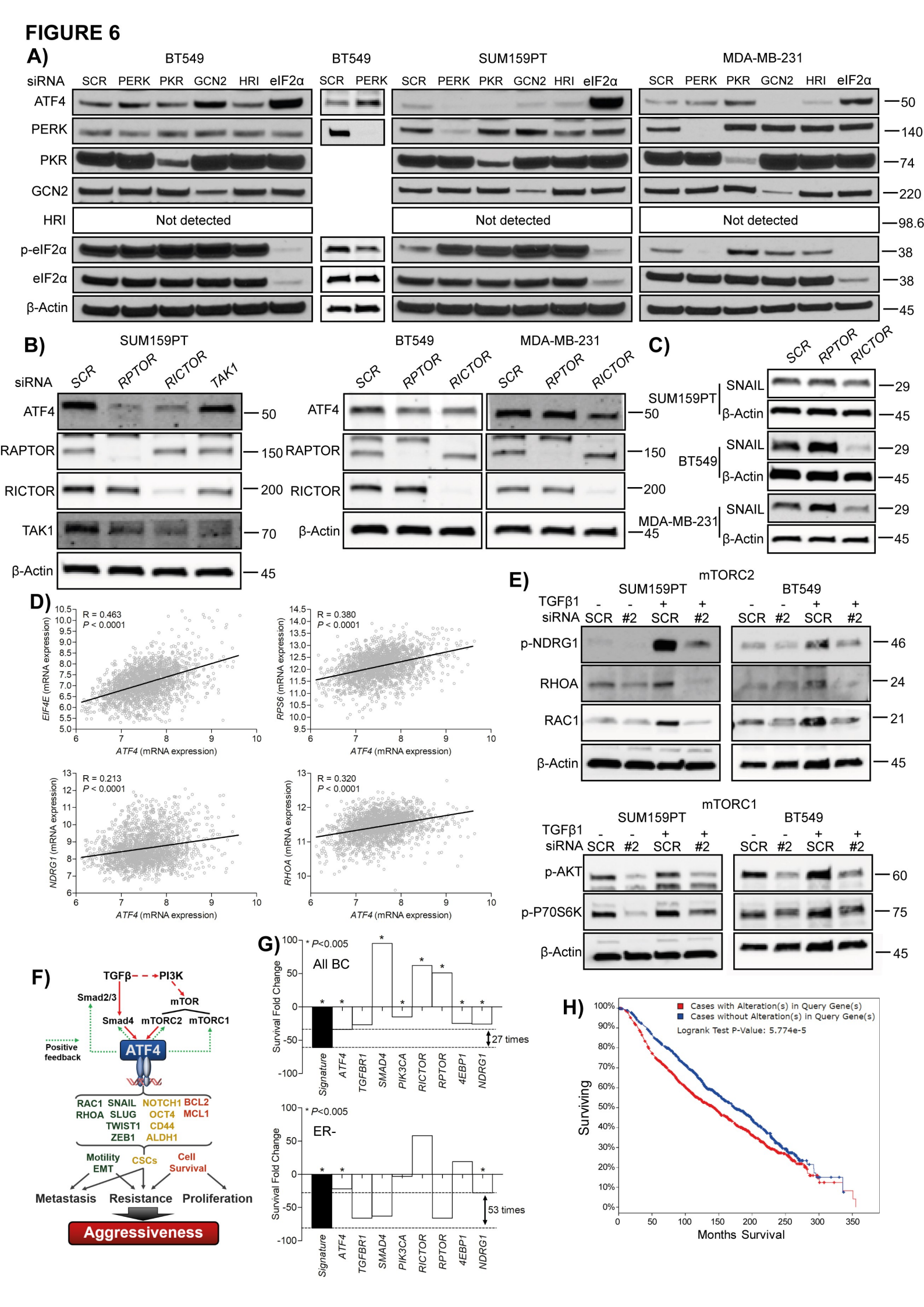
A)
BT549
BT549
SUM159PT
MDA-MB-231
siRNA SCR PERK PKR GCN2 HRI eIF2α
ATF4
PERK
PKR
GCN2
HRI
Not detected
p-eIF2α
eIF2α
β-Actin
50
140
74
220
98.6
38
38
45
B)
SUM159PT
BT549
MDA-MB-231
siRNA SCR RPTOR RICTOR TAK1
ATF4
RAPTOR
RICTOR
TAK1
β-Actin
50
150
200
70
45
C)
SCR RPTOR RICTOR
SUM159PT
BT549
MDA-MB-231
SNAIL
β-Actin
29
45
D)
R = 0.463
P < 0.0001
EIF4E (mRNA expression)
ATF4 (mRNA expression)
R = 0.380
P < 0.0001
RPS6 (mRNA expression)
R = 0.213
P < 0.0001
NDRG1 (mRNA expression)
R = 0.320
P < 0.0001
RHOA (mRNA expression)
E)
mTORC2
SUM159PT
BT549
TGFβ1
siRNA SCR #2 SCR #2 SCR #2 SCR #2
p-NDRG1
RHOA
RAC1
β-Actin
46
24
21
45
mTORC1
p-AKT
p-P70S6K
60
75
F)
TGFβ
PI3K
Smad2/3
mTOR
Smad4 mTORC2 mTORC1
Positive feedback
ATF4
RAC1 SNAIL NOTCH1 BCL2
RHOA SLUG OCT4 MCL1
TWIST1 CD44
ZEB1 ALDH1
Motility EMT
CSCs
Cell Survival
Metastasis
Resistance
Proliferation
Aggressiveness
G)
* P<0.005
All BC
Survival Fold Change
27 times
Signature ATF4 TGFBR1 SMAD4 PIK3CA RICTOR RPTOR 4EBP1 NDRG1
ER-
53 times
H)
Cases with Alteration(s) in Query Gene(s)
Cases without Alteration(s) in Query Gene(s)
Logrank Test P-Value: 5.774e-5
Surviving
Months Survival